J. Fluid Mech. (1984), vol. 143, pp. 327–350
Printed in Great Britain

Lunate-tail swimming propulsion as a problem of curved lifting line in unsteady flow. Part 1. Asymptotic theory

By H. K. CHENG AND LUIS E. MURILLO†
Department of Aerospace Engineering, University of Southern California, Los Angeles

(Received 3 January 1983 and in revised form 2 August 1983)

The asymptotic theory of a high-aspect-ratio wing in an incompressible flow is generalized to an oscillating lifting surface with a curved centreline in the domain where the reduced frequency based on the half-span is of order unity. The formulation allows applications to lightly loaded models of lunate-tail swimming and ornithopter flight, provided that the heaving displacement does not far exceed the mean wing chord. The analysis include the quasi-steady limit, in which the crescent-moon wing problem considered earlier by Thurber (1965) is solved and several aerodynamic properties of swept wings are explained.

Among the important three-dimensional and unsteady effects are corrections for the centreline curvature and for the spanwise components of the locally shed vortices. Comparison of the lift distributions obtained for model lunate tails with data computed from the doublet-lattice method (Albano & Rodden 1969) lends support to the asymptotic theory.

1. Introduction

Evolutionary changes and differentiation of a successful group to suit an environment, i.e. *adaptive radiation*, has occurred in all major phyla in the animal kingdom to produce a spectacularly diverse range of structure and behaviour (Gregory 1936; Carter 1940). Yet it is often possible to detect common adaptive mechanisms in taxonomically remoted groups, as similar solutions are evolved in response to similar or analogous selective pressures. Such is apparently the case for those nektonic animals near the top of the food pyramid where rapid and efficient movement is of paramount importance. Convergent evolution of the carangiform locomotion can be identified from many species in teleost fishes, in elasmobranchs and in cetacean mammals. Carangiform swimming is characterized by the restriction of noticeable undulation to the posterior end of the body, where the caudal fin becomes primarily responsible for thrust generation. According to Marshall (1966), the corresponding morphological adaptations are: (i) a compact, muscular, airship-like body; (ii) a pronounced necking of the body anterior to the tail; and (iii) a crescent-moon or sickle-shaped caudal fin of high aspect ratio, called the *lunate tail*. These features are illustrated by Norman & Fraser (1937), and also in figure 18 of Kramer (1960) and figure 6 of Lighthill (1969). The evolution of the carangiform mode of locomotion with the lunate tail is undoubtedly an example of the shaping influence of the ocean water, but the details regarding the precise nature of this influence have yet to be elucidated.

Lighthill (1969, 1970) has outlined the hydromechanical reasons for this convergence

† Present address: Boeing Commercial Airplane Co., Seattle, Washington 98124.

and gave an analysis of the thrust and propulsive efficiency for a 2-dimensional flat plate in heaving and pitching oscillations in an otherwise uniform stream. He also introduces a parameter that quantifies the important concept of *proportional feathering*, essential for an efficient propulsion.† In an optimization analysis, Wu (1971*b*) finds that a very high propulsive efficiency close to unity (estimated to be 0.96–0.99) is attainable in a 2-dimensional model. The performance at high efficiency may then be limited by the 3-dimensional effects which comprise the subjects of analysis in this and subsequent parts of this paper.

This paper will present the development of an asymptotic theory for oscillating lifting surfaces of high aspect ratio in a frequency range where the effect of the unsteady wake vorticity is comparable to the 3-dimensional and other corrections. Its application to the performance analysis of a model lunate tail is studied in another paper (Part 2), where an extension to the study of an ornithopter model will also be presented.

1.1. *Approach*

Numerical methods for analysing steady and unsteady 3-dimensional problems are available (see e.g. Davis 1963; Belotserkovskii 1967, 1977; Albano & Rodden 1969; Ashley & Rodden 1972) and have been employed by Chopra & Kambe (1977) and Lan (1979) in their study of the lunate-tail problem. However, the asymptotic method adopted below provides a greater simplicity in analyzing the major 3-dimensional and unsteady effects. As is well known, the classical lifting-line theory (Prandtl 1918) can be identified with the asymptotic solution to the problem of uniform steady flow past a high-aspect-ratio, unyawed, straight wing (Van Dyke 1964*a*, *b*). Lighthill (1969) points out that the analysis of relevant to the lunate-tail propulsion should treat the influence of the sweep and curvature of the planform's centreline, which is the focus of the present analysis. The results obtained are applicable also to an ornithopter model not explicitly studied here.

An extension of the classical aerodynamic theory to a curved lifting line for oscillating wings also has its own merit, more especially, its promise for a more explicit, analytical approach to the dynamic aeroelastic stability of high-aspect-ratio swept wings and rotors (cf. e.g. Weisshaar & Ashley 1973). This paper is based on materials from two unpublished works (Cheng & Murillo 1982; Murillo 1979), where much of the analyses and discussions omitted here are presented.

1.2. *Pertinent 3-dimensional studies*

The most popular among earlier extensions of Prandtl's lifting-line method is perhaps Weissinger's 1942 *ad hoc* procedure for a swept wing (see Weissinger 1947), in which the upwash correction is computed at a control point from the contributions of both the discrete trailing vortices and a bound vortex representing the wing. There is an interesting earlier study by Dorodnitsyn (1944) on wings with a curved axis (centreline) and in side slip (yaw), which draws attention to the pronounced (logarithmically large) upwash associated with the sweep; there, Weissinger's procedure was also adopted. Thurber (1965) studied a lifting surface of crescent-moon shape as an asymptotic theory for high-aspect-ratio wings, but did not solve the inner problem. Holten (1976*a*, *b*) presented formulations for high-aspect-ratio swept wings in steady and unsteady flows; the equivalence of these and those of the asymptotic theory given below is not apparent.

† This parameter controls the incidence of the wing section (at the pitch axis) with respect to the local relative wind vector.

Recently, the asymptotic theory has been extended to a straight oblique wing by Cheng (1978*a*, *b*). The asymmetric span loadings obtained from explicit analytic solutions compared well with results from a panel method (Woodward 1973) for pivoted elliptic flat plates of high aspect ratio at incidence. There has been a development of the lifting-line theory in transonic-flow research (Cheng & Meng 1979, 1980; Cook 1979; Cheng *et al.* 1981; Cheng 1982*a*, *b*), where encouraging comparison with full-potential computer solutions (Jameson & Caughey 1977) has added substantial impetus to the present approach.

1.3. *Related unsteady analyses*

Sears (1938) analyses the problem of an infinitely long vibrating ribbon with a spanwise sinusoidal amplitude variation. The work was extended by Chopra (1974) to the study of thrust and propulsive efficiency of a rectangular plate in heaving and pitching oscillations. Motivated by the lunate-tail problem, James (1975) developed a linear analysis of a high-aspect-ratio wing oscillating in an otherwise uniform stream, using the Laplace-transform technique; the study was incomplete, because the sweep and centreline curvature were not considered, and the thrust and propulsive efficiency were not analysed, and also an important part of the upwash correction was omitted (see Murillo 1979; Ahmadi 1980). However, an interesting property brought out by James (also independently by Cheng 1976) is that, in time ranges comparable to, and shorter than, the flow-transit time c_0/U (where c_0 is a reference chord and U the free-stream speed), 3-dimensional effects on an unyawed, straight, oscillating wing are much weaker than those in the steady case. This is a consequence of the *self-averaging* effect of the periodic (cross-stream) vorticity in the far wake, applicable when the characteristic wavelength $2\pi U/\omega$ is small compared with the wingspan $2b$, i.e. when $\Omega \equiv \omega b/U \gg 1$. This self-averaging effect is also expected for a swept wing, for which, however, other 3-dimensional corrections dependent on the local centreline curvature and local sweep angle are essential (Cheng 1976). In the frequency range where Ω is of order unity, the unsteady (periodic) wake vorticity will contribute as much as other 3-dimensional corrections. This represents an important range for studies of lunate-tail and ornithopter propulsions; the curved lifting-line problem will therefore be analysed mainly for this domain of $\Omega = O(1)$. We note, in passing, that Ω may be expressed as the product kA_1, where k is the reduced frequency based on the half reference chord c_0 ($k \equiv \omega c_0/2U$) and $A_1 \equiv 2b/c$ is an aspect ratio.

Thrust and propulsive efficiency of oscillating flat plates have been studied numerically by Chopra & Kambe (1977), applying Davis's (1963) kernel-function method, and by Lan (1979), applying an improved doublet-lattice method. The possibility and the condition for enhancing hydromechanical performance by the centreline sweep has not been made explicit therein. An essential point to be stressed in part 2 is that, to maintain a high efficiency, a suitable degree of (proportional) feathering should be kept at most of (if not all) the span stations. Part 2 will confirm that, by allowing a local pitch axis to control the feathering condition locally, the efficiency of a model lunate tail may increase with the averaged centreline sweep angle up to a maximum determined by the required thrust, the reduced frequency and the aspect ratio. We note in passing that, for a swimming animal, proportional feathering of the caudal fin can be realized, though not perfectly, with the help of the passive response of the flexible tail structure to local hydromechanical forces.

2. The model problem

2.1. *Assumptions and parametric requirements*

We analyse the perturbations in an incompressible irrotational flow with a uniform free stream, generated by a thin oscillating surface. The latter will be referred to alternately as the wing or the fin. The disturbances are assumed to be weak enough for the application of a linear theory. We further limit the analysis to a *planar* wing, that is, a wing with the top and bottom surfaces close enough to a reference plane that the flow conditions on the wing, and the wake can be transferred analytically to a reference plane.

The wing surfaces are assumed to be smooth with slopes no larger than $O(\epsilon)$ at all times. The planform contour is also smooth. In the limit $A_1 \to \infty$, for finite b, the projection of the leading and trailing edges will approach a single curve in the reference plane $z = 0$. The latter is called the centreline of the planform, of which the curvature is assumed to be no larger than $O(b^{-1})$. The potential solution is developed below for a high aspect ratio in a frequency range pertaining to the limit $A^{-1} \to 0$ with a fixed $\Omega \equiv kA_1 = O(1)$. Inner and outer solutions will be constructed to describe the proper limit solutions in flow regions near and far from the wing section. Taking the order of the normalized perturbation potential to be ϵ, the 3-dimensional and the unsteady corrections of interest will be of order ϵA_1^{-1} (or more precisely $\epsilon A_1^{-1} \ln A_1$ and ϵA_1^{-1}).

Physically, the trailing vortex sheet will roll up far downstream; but its effects on the outer and inner solutions are controlled directly by both the disturbances level ϵ and the aspect ratio A_1. As A_1 increases, or ϵ decreases, the region of significant roll-up will move farther and farther from the wing.

The nonlinear corrections not analysed generally are of order ϵ^2; strictly speaking, the validity of the present analysis would require $\epsilon^2 \ll \epsilon A_1^{-1}$, i.e.

$$\epsilon \ll A_1^{-1}. \tag{2.1a}$$

However, the nonlinear corrections affecting forces and propulsion are of an order higher than ϵ^2, provided that the thickness contribution can be neglected. The requirement may therefore be relaxed to

$$\epsilon = O(A_1^{-1}). \tag{2.1b}$$

The error in the linear theory resulting from the transfer of the boundary condition on a highly deflected path to the reference plane may be quite significant if ϵ is not small. Encouragingly, Chopra (1976) and Katz & Weihs (1977) have shown the influence of a large-amplitude transverse motion to be considerably weaker than suspected, especially with a low k and a transverse displacement not exceeding the fin *chord*.

Only an isolated wing model will be considered. The presence of the body and dorsal fins and their shedding of vortices may profoundly influence the lunate-tail performance, as may be anticipated from the slender-fish theory (Wu 1971*c*). This represents another aspect for future study.

2.2. *Coordinates and variables*

Figure 1(*a*) illustrates the two sets of coordinates to be employed in the following analysis: a Cartesian system (x, y, z) mainly for the outer solution and a curvilinear orthogonal system (x'', y'', z'') for the inner solution around the wing section. In the Cartesian system, the free stream is directed along the positive x-axis; the wing is

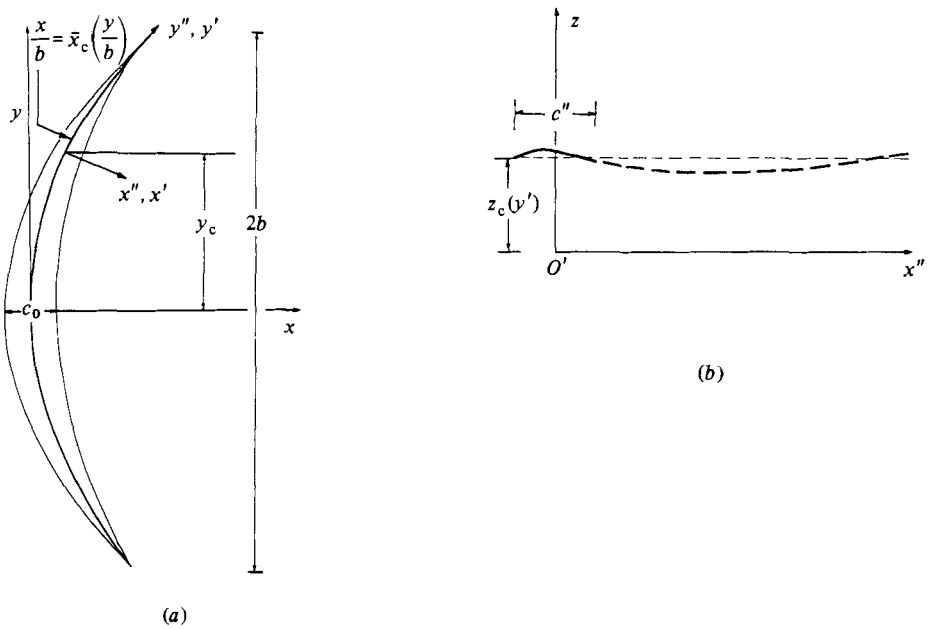

FIGURE 1. The Cartesian coordinates (x, y, z) and the orthogonal curvilinear coordinates (x'', y'', z''), the centreline of a planform, and definitions of b, c_0, c'', $x_c(y')$, z_c, y_c, etc. Note that $z_c = \epsilon b Z_c(y')$ and may be comparable to c'' in magnitude.

sufficiently close to the plane $z = 0$ that the latter may serve as a reference plane for the lifting surface and its trailing vortex sheet. The wing centreline is given by

$$\frac{x}{b} = \bar{x}_c\left(\frac{y}{b}\right). \tag{2.2}$$

Obviously, this corresponds to a lifting line and may be referred to as such. The set of normalized Cartesian variables to be used in the outer solution are $\bar{x} \equiv x/b$, $\bar{y} \equiv y/b$, $\bar{z} \equiv z/b$. In the curvilinear orthogonal system, y'' is the distance measured along the centreline and x'' the distance along the normal to the centreline at y'', oriented in the manner shown in figure 1 (*a*). The set of dimensionless variables to be used in the inner solution, with $z'' = z$, is $(x', y', z') : x' \equiv x''/c_0, y' \equiv y''/b, z' \equiv z''/c_0$. The normalized time variable is $t' = \bar{t} = \omega t$, where ω is a characteristic oscillation frequency. The value of y at the centreline for a fixed y' is y_c (cf. figure 1 *a*). In subsequent applications it will prove more convenient to employ the coordinate system $(x', \bar{y}_c, z')$ instead of (x', y', z').

For a proper description of the geometry of the high-aspect-ratio swept wing in carangiform motion we represent the wing surface ordinate $z = z_w$ as a sum of two parts:

$$z_w = \epsilon b Z_c(y', t') + \epsilon c_0 Z_w^{\pm}(x', y', t'), \tag{2.3}$$

where Z_c and $Z_w^{\pm}$ are independent of ϵ and A_1 (in the limit $\epsilon \to 0$, $A_1 \to \infty$) and the superscripts $\pm$ refer to the upper and the lower surfaces respectively. The second term of (2.3) describes a regular airfoil section with the trailing edge assumed to be sharp. The term $\epsilon b Z_c$ is introduced to allow a substantial heaving displacement of the wing

or fin section, which may be as large as the wing chord. It will define a local reference line for each span station at a given time (figure 1*b*), and has been called the wing baseline in Jones' (1972) oblique-wing study.

3. Linearized problem and inner solution

The perturbation potential ϕ in a lifting planar wing problem could be expressed in terms of a surface integral of the streamwise-velocity jump, γ say, over the wing plane $z = 0$ (Jones & Cohen 1957; Ashley & Landahl 1965). The resulting problem can be reduced to solving an integral equation for γ on the wing. We choose to analyse it, however, as a singular perturbation problem of the partial differential equation, where some of the important 3-dimensional corrections in the governing PDE and boundary conditions can be more directly identified, so that a clearer physical picture of the 3-dimensional influences may emerge.

3.1. *Equations linearized for small* ϵ

The perturbation potential of interest is a solution to the Laplace equation satisfying the impermeable boundary condition on the wing $z = z_w$ and the conditions on the trailing vortex sheet $z = z_{TV}$. The governing equations with the boundary conditions linearized for $\epsilon \ll 1$ are

$$\left(\frac{\partial^2}{\partial x^2}+\frac{\partial^2}{\partial y^2}+\frac{\partial^2}{\partial z^2}\right)\phi = 0, \tag{3.1a}$$

$$\left(\frac{\partial}{\partial z}\phi\right)_w = \frac{D}{Dt}z_w, \quad \left[\!\left[\frac{D}{Dt}\phi\right]\!\right]_{TV} = \left[\!\left[\frac{\partial}{\partial z}\phi\right]\!\right]_{TV} = 0, \tag{3.1b, c}$$

where $D/Dt \equiv \partial/\partial t + U\partial/\partial x$, $[\![\ ]\!]$ stands for the difference between the values on the upper and the lower surfaces, and the subscripts w and TV refer to the wing and the trailing vortex sheet. It is also required that ϕ be continuous in the interior and that, in the far field, excluding the vicinity of the trailing vortex sheet ($r \equiv (y^2+z^2)^{\frac{1}{2}} = O(b)$, $x \to \infty$), the gradient of ϕ tends to zero. In addition, the velocity and the pressure must remain finite at the trailing edge, fulfilling the Kutta condition.

In the curvilinear coordinates (x'', y'', z'') the linear system (3.1) becomes

$$\left[\frac{\partial^2}{\partial x''^2}+\frac{\partial^2}{\partial z''^2}-\frac{1}{h_2 R}\frac{\partial}{\partial x''}+\frac{1}{h_2}\frac{\partial}{\partial y''}\frac{1}{h_2}\frac{\partial}{\partial y''}\right]\phi = 0; \tag{3.2a}$$

$$\left(\frac{\partial}{\partial z''}\phi\right)_w = \frac{D}{Dt}z_w, \quad \left[\!\left[\frac{D}{Dt}\phi\right]\!\right]_{TV} = \left[\!\left[\frac{\partial}{\partial z''}\phi\right]\!\right]_{TV} = 0, \tag{3.2b, c}$$

where D/Dt is now expressed as

$$\frac{D}{Dt} = \frac{\partial}{\partial t} + U\cos\Lambda\frac{\partial}{\partial x''} + U\frac{\sin\Lambda}{h_2}\frac{\partial}{\partial y''},$$

where $R^{-1} \equiv d\Lambda/dy''$ is the local curvature of the centreline, h_2 is a coefficient in the metric $dx^2+dy^2+dz^2 = dx''^2+h_2^2\,dy''^2+dz''^2$ related to R and x'' as $h_2 = 1-x''/R$. Note that the local sweep angle Λ is independent of x'', and that, at the centreline

$$\tan\Lambda \equiv m = \frac{dx_c}{dy}, \quad R^{-1} = \frac{d\Lambda}{dy''} = (1+m^2)^{-\frac{3}{2}}\frac{dm}{dy}. \tag{3.3}$$

In the inner region, where the normalized variables x', y', z', t' and the perturbation velocity potential

$$\phi' \equiv \phi/\epsilon c_0 U \cos \Lambda \tag{3.4}$$

are all of *unit* order, the (linear) system (3.2) can be reduced to

$$\left(\frac{\partial^2}{\partial x'^2}+\frac{\partial^2}{\partial z'^2}\right)\phi' = -A_1^{-1} 2\kappa' \frac{\partial}{\partial x'}\phi' + \ldots, \tag{3.5a}$$

$$\left(\frac{\partial}{\partial z'}\phi'\right)_{\mathrm{w}} = V^{(0)}(x', y', t') + A_1^{-1} V^{(10)}(x', y', t') + k' V^{(01)}(x', y', t') + \ldots, \tag{3.5b}$$

$$\left[\!\left[\frac{\partial}{\partial x'}\phi'\right]\!\right]_{\mathrm{TV}} + A_1^{-1} 2m\left(\frac{\partial}{\partial y'}+m\kappa'\right)[\![\phi']\!]_{\mathrm{TV}} + 2k'\frac{\partial}{\partial t'}[\![\phi']\!]_{\mathrm{TV}} + \ldots = \left[\!\left[\frac{\partial}{\partial z'}\phi'\right]\!\right]_{\mathrm{TV}} = 0, \tag{3.5c}$$

where ... stands for the omitted terms comparable to A_1^{-2}, κ' is a normalized centreline curvature based on the half-span, and k' is a reduced frequency based on the local component velocity $U_{\mathrm{n}} \equiv U \cos \Lambda$, i.e. $\kappa' \equiv -b\,\mathrm{d}\Lambda/\mathrm{d}y'' = -b/R = -m'(y)/(1+m^2)^{\frac{3}{2}}$, $k' \equiv \omega c/2U_{\mathrm{n}} = k \sec \Lambda = A_1^{-1}\Omega \sec \Lambda$. Note that k' and A_1^{-1} are comparable under $\Omega = O(1)$, but distinguishing k' from A_1^{-1} in (3.5) should facilitate an easy identification of the genuine unsteady effects. The right-hand members of (3.5*b*) are derived from an expansion of $\mathrm{D}(z_{\mathrm{w}}/\epsilon U_{\mathrm{n}})/\mathrm{D}t$, with

$$\left.\begin{aligned} V^{(0)} &= \left(\Omega \sec \Lambda \frac{\partial}{\partial t'} + m\frac{\partial}{\partial y'}\right) Z_{\mathrm{c}} + \frac{\partial}{\partial x'} Z_{\mathrm{w}}^{\pm}, \\ V^{(10)} &= 2m\frac{\partial}{\partial y'}[-\kappa' x' Z_{\mathrm{c}} + Z_{\mathrm{w}}^{\pm}], \\ V^{(01)} &= 2\frac{\partial}{\partial t'} Z_{\mathrm{w}}^{\pm}. \end{aligned}\right\} \tag{3.6}$$

In terms of x', y' and z' the wing surfaces are located at

$$z' = 2\epsilon A_1 Z_{\mathrm{c}}(y', t') + \epsilon Z_{\mathrm{w}}^{\pm}(x', z'; y', t'). \tag{3.7}$$

Thus, transferring the boundary conditions (3.5*b*, *c*) to $z' = 0$ as in conventional planar-wing analysis would incur a relative error at the most of order ϵA_1, under (2.1*a*). On the other hand, it will be confirmed later that a displacement of the base line by an amount $z' = z'_{\mathrm{c}} = O(1)$ does not actually invalidate the present analysis to the order considered, and therefore the weaker requirement (2.1*b*) suffices and will be adopted. This becomes possible because, within the time–space domain where t', x' and z' all remain of unit order, neither the wing surfaces nor the trailing vortex sheet can depart from $z' = 2\epsilon A_1 Z_{\mathrm{c}}$ by more than $O(\epsilon)$.

3.2. *Inner expansion and reduced problems*

We assume an inner expansion for

$$\phi' = \Phi^{(0)}(x', z'; y', t') + A_1^{-1}\Phi^{(10)}(x', z'; y', t) + k'\Phi^{(01)}(x', z'; y', t') + \ldots \tag{3.8}$$

with remainders comparable to A_1^{-2}, including terms of orders $A_1^{-1}k'$ and k'^2. A weak, non-algebraic (logarithmic) dependence of the coefficients on A_1^{-1} or k' will be allowed. The inner problem thus reduces to solving the three equation systems deduced from (3.5)

I. *2-dimensional quasi-steady*:

$$\left.\begin{aligned} \nabla_1^2 \Phi^{(0)} &\equiv \left(\frac{\partial^2}{\partial x'^2}+\frac{\partial^2}{\partial z'^2}\right)\Phi^{(0)} = 0; \\ \left(\frac{\partial}{\partial z'}\Phi^{(0)}\right)_{\mathrm{w}} &= V^{(0)}, \quad \left[\!\left[\frac{\partial}{\partial x'}\Phi^{(0)}\right]\!\right]_{\mathrm{TV}} = \left[\!\left[\frac{\partial}{\partial z'}\Phi^{(0)}\right]\!\right]_{\mathrm{TV}} = 0. \end{aligned}\right\} \tag{3.9}$$

II. *3-dimensional correction*:

$$\left.\begin{aligned} \nabla_1^2 \Phi^{(10)} &= -2\kappa' \frac{\partial}{\partial x'}\Phi^{(0)}; \\ \left(\frac{\partial}{\partial z'}\Phi^{(10)}\right)_{\mathrm{w}} &= V^{(10)}, \quad \left[\!\left[\frac{\partial}{\partial x'}\Phi^{(10)}\right]\!\right]_{\mathrm{TV}} + 2m\left(\frac{\partial}{\partial y'}+m\kappa'\right)[\![\Phi^{(0)}]\!]_{\mathrm{TV}} = \left[\!\left[\frac{\partial}{\partial z'}\Phi^{(10)}\right]\!\right]_{\mathrm{TV}} = 0. \end{aligned}\right\} \tag{3.10}$$

III. *Unsteady correction*:

$$\left.\begin{aligned} \nabla_1^2 \Phi^{(01)} &= 0; \\ \left(\frac{\partial}{\partial z'}\Phi^{(01)}\right)_{\mathrm{w}} &= V^{(01)}, \\ \left[\!\left[\frac{\partial}{\partial x'}\Phi^{(01)}\right]\!\right]_{\mathrm{TV}} + 2\frac{\partial}{\partial t'}[\![\Phi^{(0)}]\!]_{\mathrm{TV}} &= \left[\!\left[\frac{\partial}{\partial z'}\Phi^{(01)}\right]\!\right]_{\mathrm{TV}} = 0. \end{aligned}\right\} \tag{3.11}$$

In the above, conditions on the wing and the trailing vortex sheet are applied at the baseline $z' = 2\epsilon A_1 Z_{\mathrm{c}} \equiv z'_{\mathrm{c}}$.

The solution $\Phi^{(0)}$ to problem I corresponds to the strip theory, and may be represented by the real part of an analytic function W of a complex variable

$$\zeta \equiv x' + \mathrm{i}(z' - z'_{\mathrm{c}}). \tag{3.12}$$

The complex velocity $\mathrm{d}W/\mathrm{d}\zeta$ satisfying (3.10) and the Kutta condition is (Munk 1922; Ashley & Landahl 1965)

$$W'(\zeta) = \frac{\mathrm{i}}{\pi}\frac{(\zeta-b)^{\frac{1}{2}}}{(\zeta-a)^{\frac{1}{2}}}\int_a^b \left|\frac{s-a}{s-b}\right|^{\frac{1}{2}} \frac{V^{(0)}(s)\,\mathrm{d}s}{s-\zeta}, \tag{3.13}$$

where a and b identify the leading and trailing edges in ζ, respectively. The arguments of $\zeta - a$ and $\zeta - b$ in $(\zeta-a)^{\frac{1}{2}}$ and $(\zeta-b)^{\frac{1}{2}}$ are restricted to the interval $(0, 2\pi)$. $V^{(0)}$ is determined by the wing geometry for the lifting problem, i.e. from (3.6) with $Z_{\mathrm{w}}^{\pm}$ evaluated as the arithmetical mean of Z_{w}^{+} and Z_{w}^{-}.

The solution for problem II may be constructed as a sum of three parts

$$\Phi^{(10)} = \phi_{(10)} + \phi^{\mathrm{P}}_{(10)} + V^{\infty}_{(10)}(z' - z'_{\mathrm{c}}). \tag{3.14a}$$

The last part allows for an upwash correction $V^{\infty}_{(10)}$ to be determined later from matching with the outer solution. The second part is the particular solution satisfying both the Poisson equation and the trailing vortex sheet conditions of (3.10):

$$\phi^{\mathrm{P}}_{(10)} = \kappa' \,\mathrm{Re}\,[\mathrm{i}(z' - z'_{\mathrm{c}})\, W] - 2m\left(\frac{\partial}{\partial y'}+m\kappa'\right)[x'\Phi^{(0)} - (z' - z'_{\mathrm{c}})\,\Psi^{(0)}] + \phi^{\mathrm{P}}_{\mathrm{H}}, \tag{3.14b}$$

where Re denotes the real part, $\Psi^{(0)}$ is the imaginary part of the complex potential $W(\zeta)$, $\phi^{\mathrm{P}}_{\mathrm{H}}$ is a Laplace solution, continuous everywhere except across the wing. The last term is introduced specifically to eliminate the unwanted singularities arising

from $-2mx'\,\partial\Phi^{(0)}/\partial y'$. The part in question has been given earlier in Cheng's (1978) oblique-wing analysis:

$$\phi_{\mathrm{H}}^{\mathrm{P}} = 2ma\frac{\partial}{\partial y'}\Phi^{(0)} + 2m\,E_{\mathrm{T}}(b-a)^{\frac{1}{2}}\frac{\mathrm{d}b}{\mathrm{d}y'}\,\mathrm{Re}\,[\mathrm{i}(\zeta-a)^{\frac{1}{2}}(\zeta-b)^{\frac{1}{2}}-\mathrm{i}\zeta\,], \tag{3.14c}$$

where E_{T} is the constant†

$$E_{\mathrm{T}} \equiv \lim_{\zeta\to b}\frac{\mathrm{i}W'(\zeta)}{(\zeta-b)^{\frac{1}{2}}}.$$

The remaining part $\phi_{(10)}$ is a Laplace solution, continuous everywhere except across the wing, and is needed for fulfillment of the wing boundary condition; it may be represented by an analytic function $W_{(10)}$ whose derivative $\partial W_{(10)}/\partial\zeta$ can be written in the same form as $W'(\zeta)$ in (3.13), with $V^{(0)}$ therein replaced by

$$\left(\frac{\partial}{\partial z}\phi_{(10)}\right)_{\mathrm{w}} = V^{(10)} - \frac{\partial}{\partial z'}\phi_{(10)}^{\mathrm{P}} - V_{(10)}^{\infty}, \tag{3.14d}$$

where $V_{(10)}^{\infty}$ is an upwash correction to be determined by the matching.

The solution for the unsteady correction, problem III, is similar to (3.14), with mt' replacing y'. The result may again be represented as a sum of three parts

$$\Phi^{(01)} = \phi_{(01)} + \phi_{(01)}^{\mathrm{P}} + V_{(01)}^{\infty}(z'-z_{\mathrm{c}}') \tag{3.15a}$$

with

$$\phi_{(01)}^{\mathrm{P}} = -2\frac{\partial}{\partial t'}[x'\Phi^{(0)} - (z'-z_{\mathrm{c}}')\,\Psi^{(0)}], \tag{3.15b}$$

and $\phi_{(01)}$ expressible in the same form as $\Phi^{(0)}$, except that $V^{(0)}$ there is replaced by

$$\left(\frac{\partial}{\partial z'}\phi_{(01)}\right)_{\mathrm{w}} = V^{(01)} - \left(\frac{\partial}{\partial z'}\phi_{(01)}^{\mathrm{P}}\right)_{\mathrm{w}} - V_{(01)}^{\infty}. \tag{3.15c}$$

We note that the addition of a homogeneous (eigen)solution to $\phi_{(01)}^{\mathrm{P}}$ in (3.15*b*) is unnecessary here, since the locations of the leading and trailing edges projected on the base line $z' = z_{\mathrm{c}}'$ are assumed to be time-independent, and $\partial\Phi^{(0)}/\partial t'$ is expected to be no more singular than $\Phi^{(0)}$.

The asymptotic behaviour of the solution at $|\zeta| \gg 1$ is essential to the matching for problems I–III, and can be expressed as

$$\Phi^{(0)} \sim \frac{\tilde{\Gamma}^{(0)}}{2\pi}(\pi-\theta) - \frac{1}{2\pi}\int_a^b \frac{\partial}{\partial s}[\![\Phi^{(0)}]\!]\,s\,\mathrm{d}s\,\mathrm{Re}\left(\frac{\mathrm{i}}{\zeta}\right) + \ldots, \tag{3.16a}$$

$$\Phi^{(10)} \sim -\kappa'\frac{\tilde{\Gamma}^{(0)}}{2\pi}(z'-z_{\mathrm{c}}')\ln|\zeta| + 2\tan\Lambda\frac{\partial}{\partial y'}\left(\cos\Lambda\frac{\tilde{\Gamma}^{(0)}}{2\pi}\right)[(z'-z_{\mathrm{c}}')\ln|\zeta| - x'(\pi-\theta)] + V_{(10)}^{\infty}(z'-z_{\mathrm{c}}') + \frac{1}{2\pi}[\![\phi_{(10)}+\phi_{\mathrm{H}}^{\mathrm{P}}]\!]_{\mathrm{TE}}(\pi-\theta) + \ldots, \tag{3.16b}$$

$$\Phi^{(01)} \sim \frac{1}{\pi}\frac{\partial}{\partial t'}\tilde{\Gamma}^{(0)}[(z'-z_{\mathrm{c}}')\ln|\zeta| - x'(\pi-\theta)] + \ldots + V_{(01)}^{\infty}(z'-z_{\mathrm{c}}') + \frac{1}{2\pi}[\![\phi_{(01)}]\!](\pi-\theta) + \ldots, \tag{3.16c}$$

† It is assumed that the edge singularities are of the square-root type. For the case in which $W'(\zeta)$ is logarithmically singular, a variant of (3.14*c*) applies (Cheng 1978). In the third-order theory for a straight, unyawed high-aspect-ratio wing, the need to choose a suitable homogeneous solution to eliminate unwanted edge singularities also arises (Kida & Miyai 1978).

where θ stands for the argument of ζ, limited to the range $(0, 2\pi)$, and $\tilde{\Gamma}^{(0)}$ is the circulation in the leading approximation, being equal to the potential jump at the trailing edge. The higher-order terms omitted are comparable to $|\zeta|^{-2}$ in (3.16*a*), and at the most unity in (3.16*b*) and (3.16*c*). The effects of these remainders as well as terms involving z_c' on the matching will be discussed later.

In the remaining part of this work, we will restrict consideration to the motion that is sinusoidal in time: $z_w = \mathrm{Re}\,(e^{i\omega t}\hat{z}_w)$, i.e.

$$Z_w = \mathrm{Re}\,(e^{it'}\hat{Z}_w), \quad Z_c = \mathrm{Re}\,(e^{it'}\hat{Z}_c). \tag{3.17}$$

The system admits a solution $\phi' = \mathrm{Re}\,(e^{i\omega t}\hat{\phi})$, with corresponding forms for coefficients $\Phi^{(0)}$, $\Phi^{(10)}$, and $\Phi^{(01)}$. Note that in terms of ζ and y', these coefficients are independent of t', even though $z_c' = \mathrm{Re}\,(e^{i\omega t}2\epsilon A_1^{-1}\hat{Z}_c)$ is time-dependent.

The perturbation pressure p' contributed by the lifting surface is, according to the linear theory,

$$p - p_\infty = \tfrac{1}{2}\rho U^2 C_p \equiv \tfrac{1}{2}\rho U_n^2 C_p' = -\rho \frac{\mathrm{D}}{\mathrm{D}t}\phi,$$

where C_p' is a pressure coefficient based on the local component dynamic pressure. For sinusoidal motion, C_p' is $\mathrm{Re}\,(e^{i\omega t}\hat{C}_p')$, and $\hat{C}_p'$ can be computed as follows:

$$\frac{\hat{C}_p'}{2\epsilon} = -\frac{\partial}{\partial x'}\Phi^{(0)} - A_1^{-1}\left[\frac{\partial}{\partial x'}\Phi^{(10)} + 2m\left(\frac{\partial}{\partial y'} + m\kappa'\right)\hat{\Phi}^{(0)}\right] - k'\left[\frac{\partial}{\partial x'}\hat{\Phi}^{(01)} + 2i\hat{\Phi}^{(0)}\right]. \tag{3.18}$$

4. Outer problem and matching

4.1. *Curved lifting line and periodic wake vorticity*

In the outer region where $\bar{x}$, $\bar{y}$ and $\bar{z}$ are of unit order, the wing and the inner region are perceived in the limit $A_1 \to \infty$ as a curved lifting line $\bar{x} = \bar{x}_c(\bar{y})$ in the wing plane $\bar{z} = 0$. The outer solution assumes the form

$$\bar{\phi} \equiv \frac{\phi}{\epsilon U c_0} = \bar{\phi}_0(\bar{x}, \bar{y}, \bar{z}, \bar{t}; \Omega) + A_1^{-1}\bar{\phi}_1(\bar{x}, \bar{y}, \bar{z}, \bar{t}; \Omega), \tag{4.1}$$

where a weak non-algebraic (logarithmic) dependence of $\bar{\phi}_1$ on A_1 is again allowed. The leading term, which vanishes far upstream and satisfies the trailing vortex sheet conditions, may be expressed in terms of the cross-stream component of the vorticity over the trailing vortex sheet, γ_{TV}, and on the wing; the latter has become a curved lifting line. Namely,

$$\bar{\phi}_0 = \bar{\phi}^L + \bar{\phi}^{TV}. \tag{4.2a}$$

with

$$\bar{\phi}^L(x, y, z, \bar{t}) = \frac{z}{4\pi}\int_{-1}^{1} \frac{\bar{\Gamma}(\bar{t}, y_1)}{(y_1 - y)^2 + z^2}\left[1 + \frac{x - x_c(y_1)}{\rho_1}\right] dy_1, \tag{4.2b}$$

$$\bar{\phi}^{TV}(x, y, z, \bar{t}) = -\frac{\Omega z}{4\pi}\iint_{S_{TV}} \frac{\dfrac{\partial}{\partial \bar{t}}\bar{\Gamma}(\bar{t} - \Omega\xi_1, y_1)}{(y_1 - y)^2 + z^2}\left[1 + \frac{x - x_1}{\rho_1}\right] dx_1\, dy_1, \tag{4.2c}$$

where $\xi_1 \equiv x_1 - x_c(y_1)$ and $\rho_1 \equiv |(x-x_1)^2+(y-y_1)^2+z^2|^{\frac{1}{2}}$; also the relation expressing the convection of the cross-stream vorticity

$$\gamma_{TV} = -U^{-1}\frac{\partial}{\partial t}\Gamma\left(t-\frac{x-x_c(y)}{U}, y\right)$$

has been used.† The overbars on x, y, and z have been omitted for convenience.

For sinusoidal motion, for which $\bar{\phi}_0 = \mathrm{Re}\,(e^{i\omega t}\hat{\phi}_0)$, and $\bar{\Gamma}_0 = \mathrm{Re}\,(e^{i\omega t}\hat{\Gamma})$, one can write

$$\hat{\phi}_0 = \hat{\phi}^L(\xi, y, z) + \hat{\phi}^{TV}(\xi, y, z), \tag{4.3a}$$

where $\xi \equiv x - x_c(y)$ is the distance from the centreline at a fixed y on the wing plane. It follows from (4.2*b*, *c*) that

$$\hat{\phi}^L(\xi, y, z) = \frac{z}{4\pi}\int_{-1}^{1}\frac{\hat{\Gamma}(y_1)}{(y-y_1)^2+z^2}\left[1+\frac{\xi+x_c(y)-x_c(y_1)}{\rho_1}\right]dy_1, \tag{4.3b}$$

$$\hat{\phi}^{TV}(\xi, y, z) = i\Omega\int_0^\infty e^{-i\Omega\xi_1}\hat{\phi}^L(\xi-\xi_1, y, z)\,d\xi_1. \tag{4.3c}$$

4.2. *The inner-limit behaviour of* $\hat{\phi}^L$ *and* $\hat{\phi}^{TV}$

The first part of $\hat{\phi}_0$, i.e. $\hat{\phi}^L$, can be more conveniently expressed, writing u for $y_1 - y$, as

$$\hat{\phi}^L(\xi, y, z) = \frac{z}{4\pi}\int_{-b-y}^{b-y}\frac{\hat{\Gamma}(y+u)}{u^2+z^2}[1+R_1^{-1}(\xi-x_c(y+u)+x_c(y))]\,du, \tag{4.4}$$

where R_1 now becomes $R_1 = |[\xi-x_c(y+u)+x_c(y)]^2+u^2+z^2|^{\frac{1}{2}}$. At the centreline ($\xi = x = 0$) the integrand is singular and non-integrable over $u = 0$. By subtracting from the integrand a suitable function with a similar behaviour, say g, the resultant integral may yield a limit as $\xi \to z \to 0$. This, together with the quadrature of g, should provide the inner-limit behaviour from $\hat{\phi}^L$ in question. The latter behaviour has in fact been determined earlier in Cheng & Meng's (1980) transonic-flow study, with x, y, z being replaced by the corresponding Prandtl–Glauert variables. For the matching to be performed subsequently, we shall transform (ξ, y, z) to $(x', y' z')$, observing in particular the relations

$$\frac{A_1\xi}{2(1+m^2)^{\frac{1}{2}}} = x' - A_1^{-1}\kappa' m^2 x'^2 + \ldots,$$

$$\hat{\Gamma}(y) = \hat{\Gamma}((y')) - 2A_1^{-1}\frac{d}{dy'}\hat{\Gamma}((y'))\,mx' + \ldots,$$

where $\hat{\Gamma}((y')) \equiv \hat{\Gamma}(y_c(y'))$, and y_c is the value of y at the centreline for a given y'. We then arrive at the inner-limit behaviour of $\hat{\phi}^L$ in terms of x', y' and z':

$$\hat{\phi}^L \sim \frac{1}{2\pi}\hat{\Gamma}((y'))[\pi-\theta] - A_1^{-1}\frac{\tan\Lambda}{\pi}\frac{d}{dy'}\hat{\Gamma}((y'))\,x'[\pi-\theta]$$

$$+ A_1^{-1}\frac{z'}{2\pi}\left(\tan\Lambda\frac{d\hat{\Gamma}}{dy'}+\frac{1}{2}\frac{d\Lambda}{dy'}\hat{\Gamma}\right)\ln|x'^2+z'^2| + A_1^{-1}z2(\Sigma+\Sigma^c), \tag{4.5a}$$

† Note that the ratio of the cross-stream and streamwise wake-vorticity components is $-U^{-1}(\partial\Gamma/\partial t)/(\partial\Gamma/\partial y) = O(\omega b/U) = O(\Omega)$.

where Σ and Σ^{c} are independent of x' and z':

$$\Sigma \equiv -\frac{1}{4\pi}\frac{\mathrm{d}\hat{\Gamma}}{\mathrm{d}y}\left\{[\ln|A_1^2(1-y^2)\sec^2\Lambda|+2]\sin\Lambda-\ln\left|\frac{1-y}{1+y}\frac{1+\sin\Lambda}{1-\sin\Lambda}\right|\right\}$$
$$+\frac{1}{4\pi}\int_{-1}^{1}\frac{\hat{\Gamma}'(y_1)-\hat{\Gamma}'(y)}{y_1-y}[1-\sin\Lambda\,\mathrm{sgn}\,(y_1-y)]\,\mathrm{d}y_1, \quad (4.5b)$$

$$\Sigma^{\mathrm{c}} \equiv -\frac{1}{8\pi}\frac{d\Lambda}{\mathrm{d}y'}\hat{\Gamma}(y)\,[\ln|A_1^2\sec^2\Lambda(1-y^2)|-2]$$
$$-\frac{1}{4\pi}\int_{-1}^{1}\left\{\hat{\Gamma}(y_1)\left[\frac{\alpha(y_1,y)}{\{[\alpha(y_1,y)]^2+(y_1-y)^2\}^{\frac{1}{2}}}-\sin\Lambda\,\mathrm{sgn}\,(y_1-y)\right]\right.$$
$$\left.-\frac{1}{2}\frac{\mathrm{d}\Lambda}{\mathrm{d}y'}\hat{\Gamma}(y)|y_1-y|\right\}\frac{\mathrm{d}y_1}{(y_1-y)^2}, \quad (4.5c)$$

with $\alpha(y_1,y)\equiv x_{\mathrm{c}}(y+u)-x_{\mathrm{c}}(y)$.

Next we consider the second part of $\hat{\phi}_0$. Expressing $\hat{\phi}^{\mathrm{L}}(\xi-\xi_1,y,z)$ in (4.3*c*) by (4.4) and interchanging the order of integration with respect to ξ_1 and u, the part in question can be expressed as

$$\hat{\phi}^{\mathrm{TV}}(\xi,y,z) = -\mathrm{i}\frac{\Omega}{\pi}z\,\mathrm{e}^{-\mathrm{i}\Omega\xi}\int_{-1}^{1}\frac{\hat{\Gamma}(y+u)}{u^2+z^2}I(\xi,p,\alpha,\Omega)\,\mathrm{d}u, \quad (4.6a)$$

where $p\equiv(u^2+z^2)^{\frac{1}{2}}$, $\alpha=\alpha(y_1,y)=x_{\mathrm{c}}(y+u)-x_{\mathrm{c}}(y)$; the function I can be arranged as a sum

$$I(\xi,p,\alpha,\Omega) = Q(\xi,p,\alpha,\Omega)+E(p,\alpha,\Omega),$$

with

$$Q(\xi,p,\alpha,\Omega)\equiv\int_{-\xi}^{0}\mathrm{e}^{-\mathrm{i}\Omega v}\left[1-\frac{v+\alpha}{[(v+\alpha)^2+p^2]^{\frac{1}{2}}}\right]\mathrm{d}v, \quad (4.6b)$$

$$E(p,\alpha,\Omega)\equiv\int_{0}^{\infty}\mathrm{e}^{-\mathrm{i}\Omega v}\left[1-\frac{v+\alpha}{[(v+\alpha)^2+p^2]^{\frac{1}{2}}}\right]\mathrm{d}v = \mathrm{e}^{\mathrm{i}\Omega\alpha}p[K_{\mathrm{a}}(\Omega p,\infty)-K_{\mathrm{a}}(\Omega p,\alpha/p)]. \quad (4.6c)$$

Note that the part E of I is independent of ξ.

In developing $\hat{\phi}^{\mathrm{TV}}$ of (4.6) for small ξ and z, we must make use of the corresponding behaviour of Q for small ξ, as well as that of E for small p. The expression for $\hat{\phi}^{\mathrm{TV}}$ in the inner limit, after changing variables (ξ,y,z) to (x',y',z'), may finally be brought down to

$$\hat{\phi}^{\mathrm{TV}} \sim \mathrm{i}k'z'\frac{\hat{\Gamma}(y_{\mathrm{c}})}{2\pi}\ln|x'^2+z'^2|-\mathrm{i}k'x'\frac{\hat{\Gamma}(y_{\mathrm{c}})}{\pi}(\pi-\theta)-\mathrm{i}k'z'(\Sigma_1^y+\Sigma_2^y), \quad (4.7a)$$

with

$$\Sigma_1^y \equiv \frac{\hat{\Gamma}(y)}{2\pi}\left[\ln|A_1^2(1-y^2)\sec^2\Lambda|-\sin\Lambda\ln\left|\frac{1-Y}{1+y}\frac{1+\sin\Lambda}{1-\sin\Lambda}\right|\right]$$
$$-\frac{\cos\Lambda}{2\pi}\int_{-1}^{1}\left\{\hat{\Gamma}(y_1)\,\mathrm{e}^{\mathrm{i}\Omega\alpha}[\alpha-(\alpha^2+(y-y_1)^2)^{\frac{1}{2}}]\right.$$
$$\left.-\hat{\Gamma}(y)\,[(y_1-y)\tan\Lambda-|y_1-y|\sec\lambda]\right\}\frac{\mathrm{d}y_1}{(y_1-y)^2}, \quad (4.7b)$$

$$\Sigma_2^y \equiv \frac{\cos\Lambda}{2\pi}\int_{-1}^{1}\frac{\hat{\Gamma}(y_1)}{(y_1-y)^2}\{E(|y_1-y|,\alpha,\Omega)+\mathrm{e}^{\mathrm{i}\Omega\alpha}\,[\alpha-(\alpha^2+(y_1-y)^2)^{\frac{1}{2}}]\}\,\mathrm{d}y_1. \quad (4.7c)$$

4.4. *Matching and discussions*

With the inner-limit behaviour of $\hat{\phi}_0 = \hat{\phi}^{\mathrm{L}} + \hat{\phi}^{\mathrm{TV}}$ furnished above and the outer-limit behaviour of $\hat{\Phi}^{(0)}$, $\Phi^{(10)}$, and $\Phi^{(01)}$ known from (3.16), the outer solution $\hat{\phi}$ and the inner solution $\hat{\Phi}$ (after being multiplied by $\cos\Lambda(y')$) may now be matched in the common domain

$$1 \ll |\zeta| \ll A_1. \tag{4.8}$$

With the exception of a line-doublet term from $\Phi^{(0)}\cos\Lambda$, two line-vortex terms from $A_1^{-1}\hat{\Phi}^{(10)}\cos\Lambda$ and $k\hat{\Phi}^{(01)}$, and also a line-source term arising from the displacement of the base line, the inner solution $\hat{\Phi}\cos\Lambda$ and the outer solution $\hat{\phi}$ can be matched to *all* terms shown in (3.16), (4.5) and (4.7), provided that

$$\left.\begin{aligned} \hat{\Gamma}((y')) &= \hat{\Gamma}^{(0)}(y')\cos\Lambda, \\ V^{\infty}_{(10)}\cos\Lambda = 2(\Sigma+\Sigma^{\mathrm{c}}), &\quad V^{\infty}_{(01)}\cos\Lambda = -\mathrm{i}(\Sigma_1^y+\Sigma_2^y). \end{aligned}\right\} \tag{4.9}$$

Thus the circulation of the lifting line $\hat{\Gamma}(y) = \hat{\Gamma}((y''))$ can be identified, and both the quasi-steady and unsteady upwash corrections $V^{\infty}_{(10)}$ and $V^{\infty}_{(01)}$ can now be determined. The terms not matched have magnitudes which are at most of order $A_1^{-1}\ln A_1$ under condition (4.8), and may be accounted for in matching carried out to a higher order.

In the far-field of $\hat{\phi}$, cf. (3.16), terms proportional to $A_1^{-1}z_{\mathrm{c}}'\hat{\Gamma}^{(0)}$ are source-like; they represent a departure from the planar-wing requirement and are in fact the nonlinear, superharmonic corrections to the outer flow. From the matching analysis it becomes apparent that, as long as $\epsilon A_1 = O(1)$, i.e. requirement (2.1*b*), the allowance for $z_{\mathrm{c}}' = O(1)$ introduces an error no larger than that for $z_{\mathrm{c}}' = O(\epsilon)$. Therefore the effects on Φ or $\hat{\Phi}$ will be no worse than $O(\epsilon^2\ln A_1)$.

The logarithmic upwash

An important difference from the classical result is the explicit presence of the logarithm of the aspect ratio in the upwash corrections, $\hat{w} \equiv A_1^{-1}V^{\infty}_{(10)} + k'V^{\infty}_{(01)}$. They can be singled out from (4.5) and (4.7) as

$$\hat{w} \sim -\frac{\ln A_1}{2\pi A_1}\left(\frac{\mathrm{d}\hat{\Gamma}}{\mathrm{d}y}2\sin\Lambda + \frac{\mathrm{d}\Lambda}{\mathrm{d}y}\hat{\Gamma}\cos\Lambda + \mathrm{i}2\Omega\hat{\Gamma}\sec\Lambda\right), \tag{4.10}$$

which represents a strong correction to the local flow angle. The first and the third terms on the right of (4.10) signify effects of the spanwise component of the locally and temporally shed vorticities. The second term give the self-induced effect of the curved bound vortex. The first term is ineffective near a symmetry plane where Λ or $\mathrm{d}\hat{\Gamma}/\mathrm{d}y$ vanishes, but prevails in the outer portion of a swept wing, since in most cases $\mathrm{d}\hat{\Gamma}/\mathrm{d}y$ becomes relatively large, or infinite, at the tip. This explains why a sweptback wing has a lesser margin to tip stall than an unswept or sweptforward wing. For the same reason, an oblique wing has an inherent rolling moment due to the induced upwash which is asymmetrically distributed in this case.

Evaluation of Σ_2

The integral Σ_2 (4.7*c*) for the unsteady upwash correction contains $E(|u|, \alpha, \Omega)$, defined by (4.6*c*), as a part of its integrand; thus the task of evaluating Σ_2 amounts to computing a double integral for each y. The procedure employed in this and subsequent studies adopts a formula developed by Watkins, Runyan & Cunningham

(1957) for the representation of the irrational fraction $t/(1+t)^{\frac{1}{2}}$ occurring in (4.6). Namely,

$$\frac{t}{(1+t^2)^{\frac{1}{2}}} \approx 1-(0.101)\,\mathrm{e}^{-0.329t}-0.899\,\mathrm{e}^{-1.4067t}-0.094\,809\,33\,\mathrm{e}^{-2.90t}\sin \pi t. \quad (4.11)$$

This gives an excellent approximation over the entire range of t, which is graphically indistinguishable from the original function. The function E may then be evaluated by a simple quadrature.

The steady state

The theory presented includes the analysis for the *steady* case ($\Omega = 0$), which furnishes a complete solution for the curved lifting-line problem considered earlier by Thurber (1965).

Weissinger's (1947) method mentioned earlier consists of replacing the wing section by a concentrated bound vortex at the quarter chord line and computes the upwash (flow angle) at the three-quarter chordline. This corresponds to an incomplete calculation of the *outer* solution $\hat{\phi}^{\mathrm{L}}$. Another difficulty also appears in Weissinger's original upwash computation procedure, which is believed to account for its failing at high A_1 as noted by Jones & Cohen (1957). In the case of straight elliptic oblique flat plate at incidence, it can be shown (Cheng & Murillo 1982) that the Weissinger method and the present theory agree if the major axis of the planform is set near the 15% chord from the leading edge, but differ considerably if the axis were located near the trailing edge.

It has been observed from an application to transonic forward-swept wings that a skew symmetry exists in the swept-angle influence on 3-dimensional corrections, which permits useful correlations of steady flows over forward-swept and aft-swept wings pertaining to an otherwise identical wing geometry (Cheng 1983). From the results established in §§3 and 4, we may find the counterpart of this skew symmetry property in the (linear) subsonic range. Examination of the 3-dimensional corrections in the steady limit reveals that they fall into two groups: one is independent of the sweep; while the other depends on $|\Lambda|$ but changes algebraic sign with the local sweep, provided that the wing bend is either zero ($Z_{\mathrm{c}} \equiv 0$) or changing sign with the sweep ($Z_{\mathrm{c}} = \operatorname{sgn}\Lambda|Z_{\mathrm{c}}|$). It is then possible to relate the solution for the forward- and aft-swept wings at corresponding points of the flow field as $\phi'_{\mathrm{FS}} = 2\phi'_{\mathrm{US}} - \phi'_{\mathrm{AS}}$, which gives

$$C'_{p\mathrm{FS}} = 2C'_{p\mathrm{US}} - C'_{p\mathrm{AS}},$$

where the subscript US refers to the unswept wing.

5. Lunate-tail models as examples: comparison with doublet-lattice solutions

This section will present lift distributions from the theory and their comparison with corresponding data from the doublet-lattice method (Albano & Rodden 1969) for a family of oscillating crescent-moon shaped wings in the regime $\Omega = kA_1 = O(1)$, including the quasi-steady limit $\Omega \to 0$. Having in mind the performance analysis in Part 2 and the importance of proportional feathering, the study will consider modes of carangiform motion with and without the proportional feathering. Solutions from Albano & Rodden's method are known to be satisfactory, except that the original procedure cannot reproduce the correction pressure jump for the *first* element adjacent to a leading edge; this aspect has been improved by Lan (1979). Nevertheless,

for the sole purpose of assessing the asymptotic theory in the surface-lift distribution, Albano & Rodden's method will suffice.

5.1. *Mode of motion and planform*

We will now consider the modelling of a caudal fin in a carangiform mode as an isolated wing, which is capable of maintaining adequate proportional feathering at each span station, at least to a first approximation. For this purpose, we will assume an oscillatory surface motion made up of *two* modes; *each* composes of pitching and heaving about its own axis, with

$$z_{\mathrm{w}} = \mathrm{Re}\{\epsilon b\, \mathrm{e}^{\mathrm{i}\omega t}[\hat{z}_{\mathrm{A}} - (x - x_{\mathrm{A}})] + \epsilon c_0\, \mathrm{e}^{\mathrm{i}\omega t}[\hat{z}_0(y') - \hat{\alpha}_0(y')\,(x' - x_0'(y'))]\}, \tag{5.1}$$

where $\hat{z}_{\mathrm{A}}$ and x_{A} are constants, with x_{A} taken to be real. For convenience the overbars in x and x_{A} have been dropped, and all terms inside the two square brackets are treated as unit-order quantities or smaller. The first mode, expressed as a linear function of the Cartesian (outer) variable x, represents the heaving and pitching motion of a *rigid* flat plate with the pitch axis at $x = x_{\mathrm{A}}$, which is usually not far from the peduncle.† The latter axis will be referred to as the major pitch axis (figure 2). The second mode, expressed in the curvilinear (inner) variables x' and y', describes the *additional* heaving–pitching motion of the fin section, with its local (curved) pitch axis set at a distance $c_0 x_0'(y')$ from the centreline (cf. thin dash–dotted curves in figure 2). The constant $\hat{z}_{\mathrm{A}}$ determines the transverse displacement of the major pitch axis of the model. A $\hat{z}_0(y') \neq 0$ would allow additional wing bending at the local hinge line $x' = x_0'$. Allowance for a spanwise variation in the local pitching amplitude and in its phase through $\hat{\alpha}_0(y')$ is essential for the exercise of proportional feathering at the local span station. For the application to an ornithopter model, one simply reorients the major axis from $x = x_{\mathrm{A}}$ to $y = 0$; the first square bracket in (5.1) should then be altered to $|y|$, with subsequent changes in (5.4)–(5.6) to be detailed in Part 2.

A parabolic shape

$$x = Ky^2 \tag{5.2}$$

will be assumed for the planform leading edge, which, for convenience, will be taken as the reference centreline $x = x_{\mathrm{c}}(y)$ in the subsequent application. To facilitate computation work, the planform trailing edge is not given in terms of x and y, but determined by the local wing chord measured normal to the y' axis:

$$c(y') = c_0(1 - y_{\mathrm{c}}^2), \tag{5.3}$$

where y_{c} is a known function of y' (figure 3).

5.2. *Wing boundary conditions: a local feathering parameter*

The functions $V^{(0)}$, $V^{(10)}$ and $V^{(01)}$ in the wing boundary condition (3.5*b*) can be calculated either from (3.6) or directly from the convective derivative of the z_{w} given by (5.1) for the model. The results can be written for an arbitrary planform as follows:

$$\left.\begin{aligned} \hat{V}^{(0)} &= -(\sec\Lambda + \hat{\alpha}_0) - \mathrm{i}\Omega\hat{H}\sec\Lambda, \quad \hat{V}^{(10)} = 2m\frac{\partial}{\partial y'}[\hat{z}_0 - \hat{\alpha}_0(x' - x_0')], \\ \hat{V}^{(01)} &= 2\mathrm{i}\,[\hat{z}_0 - x_0'\cos\Lambda - (\hat{\alpha}_0 + \cos\Lambda)\,(x' - x_0')], \end{aligned}\right\} \tag{5.4}$$

with

$$\hat{H} \equiv x_{\mathrm{c}}((y')) - x_{\mathrm{A}} - \hat{z}_{\mathrm{A}}, \tag{5.4a}$$

† The posterior body section having the minimum width, where the necking is most pronounced, is referred to as the peduncle.

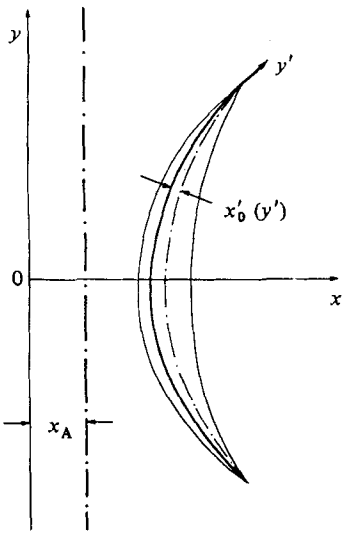

FIGURE 2. The major pitching axis (in straight dash–dotted line) and the curved local pitching axis (in thin dash–dotted curve) for the special class of the lunate-tail model analysed.

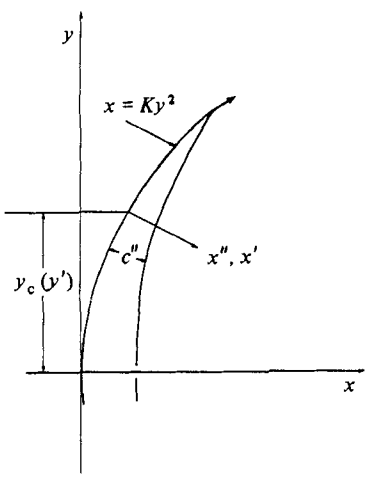

FIGURE 3. Planform and coordinates used in the lunate-tail model. Note that $c'' = c_0 c' = c_0(1-y^2)$.

where $x_c((y')) = x_c(y_c)$. Thus $V^{(0)}$ is independent of x', while $V^{(10)}$ and $V^{(01)}$ are linear in x', signifying a streamline-curvature effect. A parameter corresponding to the proportional feathering parameter of Lighthill (1969, 1970) may be identified as

$$\Theta \equiv \frac{\mathrm{i}(\sec\Lambda + \hat{\alpha}_0)}{\Omega\hat{H}\sec\Lambda}. \tag{5.5}$$

This quantity is independent of x' and can be used to eliminate $\hat{\alpha}_0(y')$ in (5.4). The factor $\sec\Lambda + \hat{\alpha}_0$ above is the sum of the maximum angles (normalized by ϵ) of the rigid-plate pitching and of the local pitching; the product $\Omega\hat{H}\sec\Lambda$ in (5.5) is the maximum heaving velocity normalized by ϵU_n at the station y' given by the rigid-plate

pitching mode.† Indeed, eliminating $\hat{\alpha}_0$ from (5.4), $\hat{V}^{(0)}$ can be brought to a form comparable to Lighthill's (1969, 1970):

$$\hat{V}^{(0)} = -\mathrm{i}\Omega\hat{H}(1-\Theta)\sec\Lambda. \tag{5.6}$$

The parameter Θ controls the departure of $V^{(0)}$ from the perfect feathering value, $\hat{V}^{(0)} \equiv 0$. The condition $-\infty < \Theta < 1$ should provide a local twist $\hat{\alpha}_0(y')$ to ensure the proper incidence relative to the trajectory of the hinge for generating a positive thrust component from the Joukowski lift (at all times, according to the quasi-steady local strip theory).

The Θ considered in most examples in §5.4, and in Part 2, falls in the range $0 < \Theta < 1$; *for simplicity*, its value is taken to be *uniform spanwise*. Examples with a fixed Θ will be referred to hereinafter as the 'feathering cases'. As contrasting examples, cases with $\hat{\alpha}_0 = \hat{z}_0 = 0$, corresponding to a rigid flat plate in pitch, will also be studied. They will be referred to as the 'rigid cases'. It must be emphasized that Θ of (5.5) and (5.6) determine the wing upwash $\mathrm{D}z_\mathrm{w}/\mathrm{D}t$ only in the limit $A_1^{-1} \to k \to 0$. The approach to a more genuine perfect-feathering condition corresponding to $\mathrm{D}z_\mathrm{w}/\mathrm{D}t \equiv 0$ would call for additional 3-dimensional and unsteady constraints ($V^{(10)} = V^{(01)} = 0$).

5.3 *Surface lift distributions and circulation*

The analytic base for the hydromechanical performance is the surface-lift distribution, or the C'_p jump, calculated from jumps of $\Phi^{(0)}$, $\Phi^{(10)}$ and $\Phi^{(01)}$ according to (3.18). From the lift distribution one can determine the surface contributions to the thrust and the power as well as the thrust component of the leading-edge suction.

For the mode shape (5.1), the jumps in Φ and their derivatives in question can be expressed in terms of the surface coordinates (x', y_c), the local chord c', local sweep and curvature Λ and κ', and the values of $\hat{\alpha}_0$ or Θ, x'_0, $\hat{z}_0$ etc., and also the major axis locations x_A and the $\hat{z}_\mathrm{A}$, which prove to be crucial for hydrodynamic performance. They are given explicitly in (5.7) in Cheng & Murillo (1982).

To compute $V^\infty_{(10)}$ and $V^\infty_{(01)}$, the leading-order circulation $\hat{\Gamma}(y) = \hat{\bar{\Gamma}}^{(0)}((y_\mathrm{c}))\cos\Lambda$, with $\hat{\bar{\Gamma}}^{(0)} = -\pi\hat{V}^{(0)}c'$, is required. The latter can be computed alternatively as

$$\hat{\bar{\Gamma}}^{(0)}(y) = \mathrm{i}\pi\Omega(1-\Theta)\hat{H}c', \quad \hat{\bar{\Gamma}}^{(0)}(y) = -\pi(1+\alpha_0\cos\Lambda)c' + \mathrm{i}\pi\Omega\hat{H}c'. \tag{5.8a, b}$$

The distributions $\hat{\Gamma}(y)$ for the feathering and rigid cases can be directly inferred from (5.8*a*, *b*) with the substitution of $\hat{H}c' = (Ky^2 - x_\mathrm{A} - \hat{z}_\mathrm{A})(1-y^2)$ and $\hat{\alpha}_0 \equiv 0$ respectively. The contrast of the two mode shapes is significant (especially for the carangiform prototypes having small $|x_\mathrm{A}|$ and $|z_\mathrm{A}|$) because the real part of $\hat{\bar{\Gamma}}^{(0)}$ is seen to dominate in a rigid case but is relatively small in a feathering case.

5.4. *Results and comparison*

For the comparison study, the surface-lift distributions $[\![C'_p]\!]$, have been computed as functions of x' and $y_\mathrm{c}(y')$ from (3.18) for several sets of A, K, Ω, x_A, x'_0, $\hat{z}_0$, $\hat{z}_\mathrm{A}$, etc., corresponding to the mode shape to be studied in the subsequent performance analysis. In all cases examined below, we take $\hat{z}_\mathrm{A} = \hat{z}_0 = 0$, and the local pitch axis is set at the local quarter-chord point, i.e. at $x' = \frac{1}{4}c'$. To facilitate comparison with the doublet-lattice method, this chordwise distribution at a fixed y_c is transferred analytically to a neighbouring wing section of fixed y as function of $\tilde{x} \equiv (x - x_\mathrm{LE})/(x_\mathrm{TE} - x_\mathrm{LE})$. The final result of $[\![C_p]\!] = [\![C'_p]\!]\cos^2\Lambda_\mathrm{c}$, where

† The parameter Θ may be seen to be proportional to the amplitude of the tail pitching angle and inversely proportional to the tail-beat frequency and the heaving amplitude.

$\Lambda_c = \Lambda(y') = \Lambda((y_c))$, will be compared with the corresponding data from the doublet-lattice method.

The doublet-lattice method of Albano & Rodden (1969) gives numerical solutions to the linearized compressible-flow equation for an oscillatory wing. In its application, the half-wing of a lifting surface with bilateral symmetry is divided into N_s strips, each of which is subdivided into N_c intervals chordwise, giving a total of $N_s \times N_c$ panels or elements. The lift distribution over each panel is represented by a line of doublet singularity (for the acceleration potential) along the *quarter-chord* line of the panel. The impermeability condition of the wing is satisfied by the induced velocity computed from the doublet lattice (acceleration potential) at a 'receiving point' identified with the midpoint at the three-quarter chord line of each panel, giving $N_s \times N_c$ algebraic equations for the determination of the lift on each panel. The algorithm is implemented by a second-degree polynomial fit for a factor in a kernel function for each panel, and by the use of the Watkins *et al.* (1959) representation, cf. (4.14), to aid the evaluation of the kernel. The available program limits the total number of panels ($N_s \times N_c$) to 100. Owing to this limitation and to the polynomial approximation, the adequacy of this numerical method appears to be uncertain for a high-aspect-ratio wing (according to Albano & Rodden 1969). The proper combination of N_s and N_c for achieving a maximum accuracy is also unclear. To obtain the pressure coefficient from numerical solutions, we divide the lift of the individual panel from the program by its area and interpret it to be the pressure *at* the midpoint of the *quarter-chord* line, as successfully practiced by Albano & Rodden (1969).

Rigid plate at incidence: $\hat{\alpha}_0 \equiv 0, \Omega \to 0$

Figure 4 represents results for the normalized chordwise pressure difference $-[\![\hat{C}_p]\!]/2\epsilon$ versus x for a rigid plate in the quasi-steady limit $\Omega \to 0$, corresponding to a flat (zero-camber) lunate-shaped wing at incidence in a *steady* stream. The results are computed for a parabolic leading edge with an average sweep parameter $K = 0.50$, and an aspect ratio $A_1 = 15$; the major axis is located at $x_A = -0.20$. The distributions determined from the theory (in solid curves) and from the doublet-lattice method (in open circles) are shown for five span stations $y = 0.025, 0.175, 0.375, 0.575$ and 0.875. The uniform agreement of the latter with data from the Albano–Rodden code is clear. For this data set, 20 uniformly spaced spanwise stations over the half-span are used in the Albano–Rodden code, i.e. $N_s = 20$; only five chordwise panels ($N_c = 5$) are left for each spanwise strip. One must note, nevertheless, that the experience with the code for $\Omega = 0$ described above does not fully reflect the property of the Albano–Rodden code since the code reduces virtually to the vortex-lattice method (Hedman 1965) in this limit.

Rigid-plate pitching: $\hat{\alpha}_0 \equiv 0$, $\Omega = 1$

A more critical comparison with the doublet-lattice method is given in figure 5, where the real and imaginary parts of the pressure differences on a lunate-shaped wing in pitching oscillation are presented. The planform and mode shape are identical with those of the preceding figure except for a non-vanishing reduced frequency, $\Omega = 1$. As in the preceding figure, the strip theory (in dashes) gives a higher $-\mathrm{Re}\,[\![C_p]\!]$ than the doublet-lattice method (in open circles) near the root ($y \to 0$), and a lower $-\mathrm{Re}\,[\![C_p]\!]$ near the tip ($y \to 1$). The agreement of the doublet-lattice data with theory (in full curves) is good with a slight deterioration in the imaginary parts near the tip ($y = 0.875$ and 0.975). Since the local wing chord vanishes towards the tip, the aspect

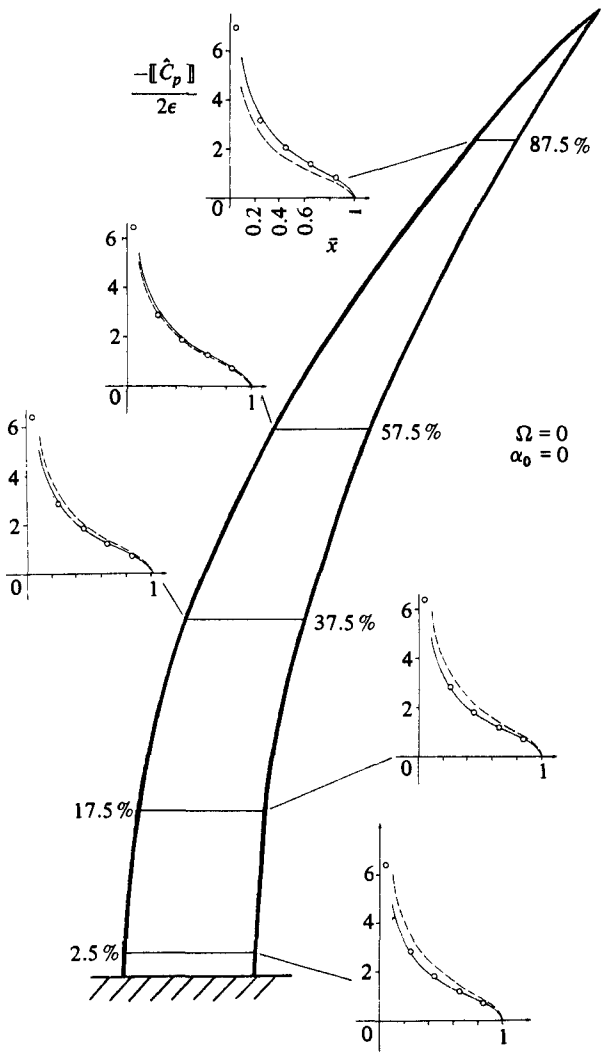

FIGURE 4. Chordwise lift distributions at five span stations computed from the theory (full curves), from the quasi-steady strip method (dashed), and from the Albano–Rodden (doublet-lattice) method (open circles) for a rigid lunate-shaped plate in the quasi-steady limit: $\hat{\alpha}_0 = \Omega = 0$, $K = 0.50$, $A_1 = 15$, $x_A = -0.2$, $\hat{z}_A = \hat{z}_0 = 0$.

ratio of the individual wing panels at each span station in the doublet-lattice method becomes progressively higher as one moves towards the tip; this invariably invalidates the polynomial representation in the kernel in the Albano–Rodden method indicated earlier. In addition, the errors resulting form the replacement of the smooth lunate planform by a triangular panel at the tip in the numerical method may become quite large.

Feathering case: $\Theta = 0.60$, $\Omega = 1$

We obtain solutions from the theory and from the doublet-lattice method for the same lunate planform ($K = 0.50$, $A_1 = 15$) and a mode shape pertaining to $\hat{z}_A = \hat{z}_0 = 0$, $x_A = -0.2$, $\Omega = 1$, with the feathering parameter set at $\Theta = 0.60$. The

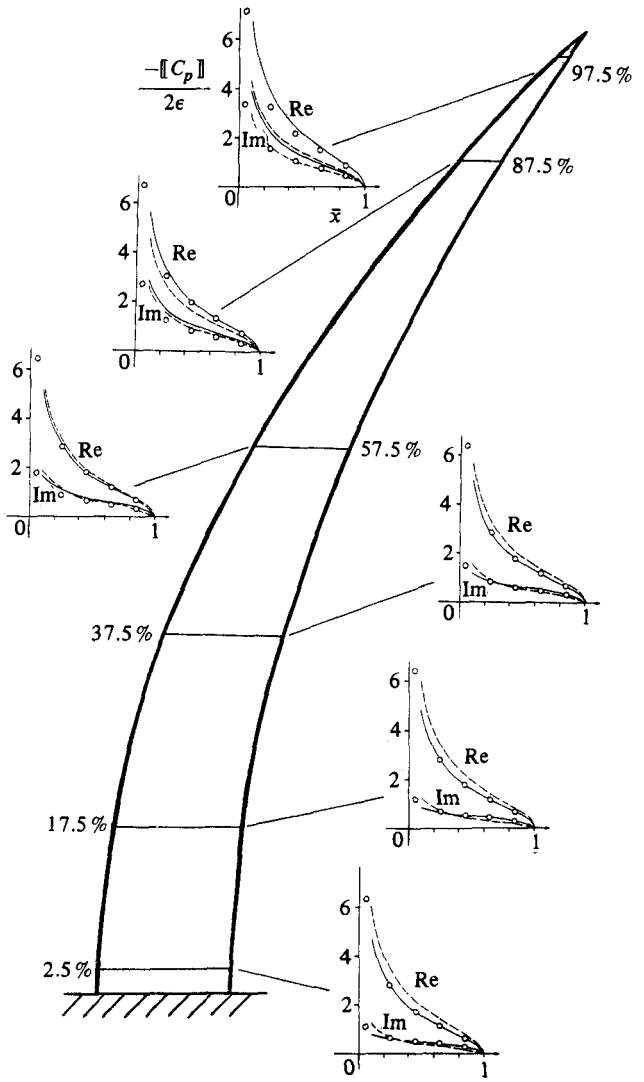

FIGURE 5. Chordwise lift distributions at six span stations computed from the theory (full curves), from the quasi-steady strip method (dashes) and from the Albano–Rodden method (open circles) for a rigid lunate-shaped plate in pitching oscillation: $\alpha_0 = 0, \Omega = 1, K = 0.50, A_1 = 15, x_A = -0.20, \hat{z}_A = \hat{z}_0 = 0$.

solid curves of figure 6 show the theoretical chordwise pressure differences for this feathering case at five span stations, where agreement with the Albano–Rodden code (open circles) is found to vary from good to fair. Departure is noticeable at the two stations close to the plane of symmetry ($y = 0.025, 0.137$), where the improvement of the present theory over the strip method (shown in dashes) remains evident, however.

A source of the noticeable discrepancy could come from an inadequacy of the asymptotic results in approximating the real part of the lift distribution at the two inner span stations, which is itself quite small. Another, most likely, source for the discrepancy may be traced to the inaccuracy in prescribing the wing boundary condition for the Albano–Rodden code, which calls for a transformation of the

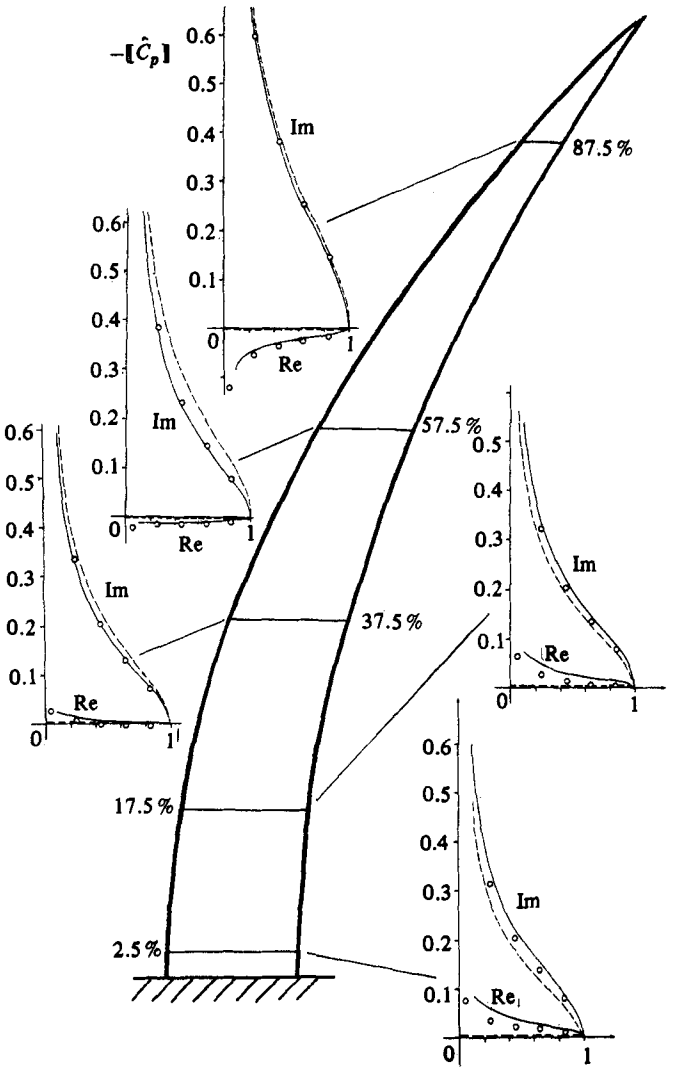

FIGURE 6. Chordwise lift distributions at six span stations computed from the theory (full curves), from the quasi-steady strip method (dashes) and from the Albano–Rodden method (open circles) for an oscillating lunate-tail model: $\Theta = 0.60$, $\Omega = 1$, $K = 0.50$, $x_0' = 0.25$, $x_A = -0.20$, $\hat{z}_A = \hat{z}_0 = 0$, $A_1 = 15$.

curvilinear to the Cartesian coordinates. In the transformation, terms of order A_1^{-2} were omitted. (A similar discrepancy is not found in the rigid-plate cases, for which the prescribed boundary values are exact.) Results obtained for examples identical with those of figures 4–6 except for a lower aspect ratio $A_1 = 10$ (not shown) indicate that similar agreement with the vortex-lattice method is found and that the improvement over the strip method is much more significant in this case.

6. Summary and discussion

The asymptotic theory of a high-aspect-ratio wing (Prandtl 1918; Van Dyke 1964*a*, *b*) has been generalized to an oscillating lifting surface with a curved axis in a low-frequency domain $\Omega \equiv kA_1 = O(1)$, where the flow next to the wing section is

nearly quasi-steady, while the velocity induced by the unsteady wake vorticities is as large as that induced by the trailing vortex system in Prandtl's lifting-line theory. Application to model problems of lunate tail yields explicit surface-lift distributions in reasonable agreement with corresponding data from the doublet-lattice method (Albano & Rodden 1969) in most span stations. Limited discrepancies are found on the tip and root sides in some cases and are believed to be traceable to errors in prescribing input data to the Albano–Rodden code for certain mode shape. They are not large enough to invalidate the conclusions on the comparison study.

The theory is limited to a weakly perturbed potential flow and a nearly planar lifting surface with a centreline curvature no stronger than $O(b^{-1})$. Allowing minor modifications, results in §§5.1–5.3 are applicable to ornithopter models for certain birds and insects. The theory presented in §§3 and 4 is sufficiently explicit, yet general, to promise an analytical attack of the 3-dimensional effects on the dynamics and aeroelasticity of high-aspect-ratio swept wings and its extension to rotors. In the special limit $\Omega \to 0$, the work completes the solution to the crescent-moon wing problem initiated by Thurber (1965); it also provides a basis for studying the limitation of Weissinger's (1947) '$\frac{3}{4}$-method' for swept wings. From the explicit results, symmetry properties of the 3-dimensional corrections with respect to the local sweep angle $\Lambda(y')$ in the steady case are noted, by which aerodynamic data of the sweptforward wing can be correlated with corresponding data of sweptback and unswept wings. Among the essential ingredients distinguishing the present work from a conventional lifting-line analysis are the corrections in the equations governing the *inner* problem due to both the (local) centreline curvature and the cross-stream component of the (locally) shed vorticity. In the context of a steady or quasi-steady flow, the logarithmic upwashes noted in §4.4 explain the tip-stall tendency of a swept-back wing as well as the rolling tendency of an oblique wing.

Records of animals swimming and flying do not strongly support the assumption of the purely sinusoidal oscillation at a *single* frequency. In principle, the solution for a more general motion could be generated from a weighted inverse Fourier transform of the present result in time, which is limited in this study, however, to the low frequency range.

Considering a straight, unyawed, flapping wing, Jones (1980) noted an interesting analogy between the problem of minimizing the wing-flapping energy and the problem of minimizing the induced drag for wings in steady motion having a given lift and root-bending moment. Implicit in Jones' work is the assumption of the quasi-steady limit. Estimates from wing-beat frequencies and flight speeds of common birds indicate, however, that $\Omega \equiv kA_1$ belongs to the unit-order range in many cases. Interestingly, the subsequent analysis in Part 2 will show that propulsive performance is generally enhanced at an $\Omega \neq 0$.

A serious limitation of the present model is the assumption of the nearly planar wing and wake. This remains to be improved. The influence of vorticities shed from the body or dorsal fins ahead of the caudal fin has not been considered, which may also affect the flow and performance of the caudal fin significantly.

This work is supported by the National Science Foundation Engineering Division, Contract no. CME-7926003. Partial support by the Office of Naval Research, Fluid Dynamics Branch is also acknowledged.

It is our pleasure to acknowledge the valuable comments and advice received from Sir James Lighthill and Drs R. T. Jones and T. Y. T. Wu. Suggestions and assistance

from Drs E. Albano, R. H. Edwards, G. Spedding, B. A. Troesch and D. Weihs were extremely helpful. Our computational study could not have been completed without the excellent and extensive numerical work performed by Mr G. Karpouzian.

REFERENCES

AHMADI, A. R. 1980 Ph.D. dissertation, MIT.

ALBANO, E. & RODDEN, W. P. 1969 *AIAA J.* **7**, 279–285.

ASHLEY, H. & LANDAHL, M. 1965 *Aerodynamics of Wings and Bodies.* Addison-Wesley.

ASHLEY, H. & RODDEN, W. P. 1972 *Ann. Rev. Fluid Mech.* **4**, 431–472.

BATCHELOR, G. K. 1967 *An Introduction to Fluid Dynamics*, pp. 510, 523. Cambridge University Press.

BELOTSERKOVSKII, S. M. 1967 *The Theory of Thin Wings in Subsonic Flow.* Plenum.

BELOTSERKOVSKII, S. M. 1977 *Ann. Rev. Fluid Mech.* **9**, 469–494.

CARTER, G. S. 1940 *A General Zoology of the Invertebrates*, chap. 23. London.

CHENG, H. K. 1976 *Univ. S. Calif., Dept Aerospace Engng Rep.* USCAE 133.

CHENG, H. K. 1978*a* *AIAA J.* **16**, 1211–1213.

CHENG, H. K. 1978*b* *Univ. S. Calif., Dept Aerospace Engng Rep.* USCAE 135.

CHENG, H. K. 1982*a* The transonic flow theories of high and low aspect ratio wings. In *Physical and Numerical Aspects of Aerodynamic Flows* (ed. T. Cebeci), Springer-Verlag.

CHENG, H. K. 1982*b* In *Transonic, Shock and Multidimensional Flows* (ed. R. E. Meyer), pp. 107–145. Academic.

CHENG, H. K. 1983 Transonic aerodynamics of forward swept wings analyzed as a lifting-line problem. In *Proc. Intl Forward-Swept Wing Aircraft Conf. Bristol University*, 24–26 *March* 1982.

CHENG, H. K., CHOW, R. & MELNIK, R. E. 1981 *Z. angew. Math. Phys.* **32**, 481–496.

CHENG, H. K. & MENG, S. Y. 1979 *AIAA J.* **17**, 121–124.

CHENG, H. K. & MENG, S. Y. 1980 *J. Fluid Mech.* **97**, 531–556.

CHENG, H. K., MENG, S. Y., CHOW, R. & SMITH, R. 1981 *AIAA J.* **19**, 961–968.

CHENG, H. K. & MURILLO, L. E. 1982 *Univ. S. Calif. Dept Aerospace Engng Rep.* USCAE 139.

CHOPRA, M. E. 1974 In *Swimming and Flying in Nature*, vol. 2 (ed. T. Y. T. Wu *et al.*).

CHOPRA, M. G. 1976 *J. Fluid Mech.* **74**, 161–181.

CHOPRA, M. G. & KAMBE, T. 1977 *J. Fluid Mech.* **79**, 49–69.

COOK, L. P. 1979 *Q. Appl. Maths* **32**, 178–202.

DAVIS, D. E. 1963 *Aero. Res. Counc. R & M* 3409.

DORODNITSYN, A. A. 1944 *Prikl. Mat. Mech.* **8**, 33–64.

GREGORY, W. K. 1936 *Biol. Rev.* **11**, 310.

HEDMAN, S. G. 1965 *Aero. Res. Inst. Sweden Rep.* 105.

HOLTEN, T. VAN 1976*a* *J. Fluid Mech.* **77**, 561–599.

HOLTEN, T. VAN 1976*b* Asymptotic theory of swept wings. *Delft Univ. Dept. Aerospace Engng Rep.*

JAMES, E. C. 1975 *J. Fluid Mech.* **70**, 735–771.

JAMESON, A. & CAUGHEY, D. A. 1977 *New York Univ. ERDA Rep.* C00-3077-140.

JONES, R. T. 1972 *AIAA J.* **10**, 171–176.

JONES, R. T. 1980 *Aero. J. R. Aero. Soc.* July, 214–217.

JONES, R. T. & COHEN, D. 1957 Aerodynamics of wings at high speed. In *Aerodynamic Components of Aircraft at High Speed* (ed. A. F. Donovan & H. R. Lawrence), pp. 1–236. Princeton University Press.

KÁRMÁN, T. VON & BURGERS, J. M. 1934 General aerodynamic theory. In *Aerodynamic Theory* (ed. W. F. Durand), vol. 2, div. E.

KATZ, J. & WEIHS, D. 1978 *J. Fluid Mech.* **88**, 485–487.

KIDA, T. & MIYAI, T. 1978 *Z. angew. Math. Phys.* **29**, 519–607.

KRAMER, M. O. 1960 *J. Am. Soc. Nav. Engng* **72**, 25–34.

LAN, C. E. 1979 *J. Fluid Mech.* **93**, 747–765.

LIGHTHILL, M. J. 1960 *J. Fluid Mech.* **9**, 305–317.

LIGHTHILL, M. J. 1969 *Ann. Rev. Fluid Mech.* **1**, 413–466.

LIGHTHILL, M. J. 1970 *J. Fluid Mech.* **44**, 265–301.

LIGHTHILL, M. J. 1975 *Mathematical Biofluiddynamics.* SIAM.

MARSHALL, N. B. 1966 *The Life of Fishes.* The Universe Books.

MUNK, M. M. 1922 *NACA Rep.* 142.

MURILLO, L. E. 1979 Hydromechanical performance of lunate tails analyzed as a lifting-line problem in unsteady flow. Dissertation, University of Southern California.

NORMAN, J. R. & FRASER, F. C. 1937 *Giant Fishes, Whales and Dolphines.* Putnam.

PRANDTL, L. 1918 *Nachr. Ges. Wiss. Gött. Math.-Phys. Klass.*, 451–477.

SEARS, W. R. 1938 In *Proc. 5th Int. Congr. Appl. Mech.* pp. 483–487.

THURBER, J. K. 1965 *Commun. Pure Appl. Maths* **18**, 733–750.

VAN DYKE, M. D. 1964*a* *Perturbation Methods in Fluid Mechanics*, p. 176. Academic. [See also annotated edition; Parabolic, 1975.]

VAN DYKE, M. D. 1964*b* *Q. Appl. Maths Mech.* **28**, 90–101.

WATKINS, C. C., RUNYAN, H. L. & CUNNINGHAM, H. J. 1959 *NASA TR R*-48.

WEISSHAR, T. A. & ASHLEY, H. 1973 *J. Aircraft.* **10**, 586–594.

WEISSINGER, J. 1947 *NACA Tech. Memo.* 1120. [Transl. FB 1553, Berlin–Adlershof 1942.]

WOODWARD, F. A. 1973 *NASA CR* 2228, parts I and II.

WU, T. Y. T. 1971*a* *J. Fluid Mech.* **46**, 337–355.

WU, T. Y. T. 1971*b* *J. Fluid Mech.* **46**, 521–544.

WU, T. Y. T. 1971*c* *J. Fluid Mech.* **46**, 545–568.